Harmful Algae 85 (2019) 101698

Contents lists available at ScienceDirect

Harmful Algae

journal homepage: www.elsevier.com/locate/hal

Combination of ocean acidification and warming enhances the competitive advantage of *Skeletonema costatum* over a green tide alga, *Ulva linza*

Guang Gao[a,b], Qianqian Fu[a], John Beardall[c], Min Wu[a], Juntian Xu[a,d,e,*]

[a] Jiangsu Key Laboratory of Marine Bioresources and Environment, Jiangsu Ocean University, Lianyungang, 222005, China
[b] State Key Laboratory of Marine Environmental Science, Xiamen University, Xiamen, 361005, China
[c] School of Biological Sciences, Monash University, Clayton, Victoria 3800, Australia
[d] Co-Innovation Center of Jiangsu Marine Bio-industry Technology, Lianyungang 222005, China
[e] Jiangsu Key Laboratory of Marine Biotechnology, Jiangsu Ocean University, Lianyungang 222005, China

ARTICLE INFO

Keywords:
Green tide
Interspecific competition
Ocean acidification
Photosynthesis
Red tide
Warming

ABSTRACT

Red tide and green tide are two common algal blooms that frequently occur in many areas in the global oceans. The algae causing red tide and green tide often interact with each other in costal ecosystems. However, little is known on how future CO_2-induced ocean acidification combined with temperature variation would affect the interaction of red and green tides. In this study, we cultured the red tide alga *Skeletonema costatum* and the green tide alga *Ulva linza* under ambient (400 ppm) and future CO_2 (1000 ppm) levels and three temperatures (12, 18, 24 °C) in both monoculture and coculture systems. Coculture did not affect the growth rate of *U. linza* but significantly decreased it for *S. costatum*. Elevated CO_2 relieved the inhibitory effect of *U. linza* on the growth of *S. costatum*, particularly for higher temperatures. At elevated CO_2, higher temperature increased the growth rate of *S. costatum* but reduced it for *U. linza*. Coculture with *U. linza* reduced the net photosynthetic rate of *S. costatum*, which was relieved by elevated CO_2. This pattern was also found in Chl *a* content, indicating that *U. linza* may inhibit growth of *S. costatum* via harming pigment synthesis and thus photosynthesis. In monoculture, higher temperature did not affect respiration rate of *S. costatum* but increased it in *U. linza*. Coculture did not affect respiration of *U. linza* but stimulated it for *S. costatum*, which was a signal of responding to biotic and/abiotic stress. The increased growth of *S. costatum* at higher temperature and decreased inhibition of *U. linza* on *S. costatum* at elevated CO_2 suggest that red tides may have more advantages over green tides in future warmer and CO_2-enriched oceans.

1. Introduction

Red tides are a form of harmful algal blooms that refers to water discoloration caused by phytoplankton including dinoflagellates, diatoms and cyanobacteria (Anderson, 2009). Over the last several decades, the proliferation of harmful algal blooms and their impacts on marine organism and human health have attracted considerable concern. The toxins produced by harmful algae can kill marine animals, such as fish, bivalves and seabirds (Turner et al., 1998; Shumway et al., 2003; Kirkpatrick et al., 2004). For instance, active red tides caused by *Karenia brevishave* have been estimated to kill up to 100 tons of fish per day in Florida (Kirkpatrick et al., 2004). Harmful algal blooms can also pose health risks to humans by consumption of contaminated seafood and respiratory exposure to aerosolized toxins (Morabito et al., 2018). Marine algal toxins are responsible of more than 60, 000 intoxication incidents per year worldwide, leading to an overall 1.5 % mortality (Bourne et al., 2010). Red tides generally occur in warmer waters with poor circulation, but a global increase in the geographic extent, frequency, and magnitude of these events due to transport of algal species via ship ballast waters, increased nutrient loading, and global warming over the last two decades has been documented (Anderson, 2009; Bibak and Hosseini, 2013).

Meanwhile, excessive growth of macroalgae along the shores of industrialized countries has been noted since the 1970's (Fletcher, 1996) and are now termed "green tides". Green tides occur mainly in the North Temperate Zone, with the United States, Europe and the Asia-Pacific areas the most seriously affected (Ye et al., 2011). Large-scale green tides, consisting of *Ulva* species, have regularly invaded the coastal zones of the western Yellow Sea in China since 2007 (Zhang et al., 2019). Due to their frequent occurrence, the consequences of green tides have drawn considerable attention. Apart from the negative influence on aesthetics and tourism, green tides could lead to the

* Corresponding author at: Jiangsu Key Laboratory of Marine Bioresources and Environment, Jiangsu Ocean University, Lianyungang, 222005, China.
E-mail address: jtxu@jou.edu.cn (J. Xu).

https://doi.org/10.1016/j.hal.2019.101698
Received 6 July 2019; Received in revised form 22 October 2019; Accepted 23 October 2019
Available online 14 November 2019
1568-9883/

mortality of marine animals and thus substantial aquaculture losses mainly due to hypoxia or anoxia in the waters caused by decomposition of thalli (Smetacek and Zingone, 2013; Ye et al., 2011).

Although the areas where microalgal and macroalgal blooms occur often overlap, these two kinds of blooms do not occur together at the same time (Smith and Horne, 1988; Fong et al., 1993; Xia et al., 2009). There are two possible reasons for this. Firstly, microalgae and macroalgae would compete with each other for resources, such as nutrients, light, space, etc. (Besterman and Pace, 2018). In addition, the negative correlation in biomass between microalgae and macroalgae could be attributed to allelopathic interactions. *U. rigida,* both in the form of fresh thalli and dry powder, has been show to exert inhibitory effects on the growth of the benthic dinoflagellate *Ostreopsis* cf. *ovata* (Accoroni et al., 2015). The fresh tissue, dry powder and aqueous extracts of *U. pertusa* also inhibited the growth of the raphidophyte *Heterosigma akashiwo* and the dinoflagellate *Alexandrium tamarense* (Wang et al., 2007). Compared to the allelopathic effect of macroaglae on microalgae, studies regarding the allelopathic effect of microalgae on macroalgae are relatively rare. The growth rate of *U. pertusa* was inhibited by 7.24 % when cultured with *Heterosigma akashiwo* (Nan et al., 2004). However, the opposite finding was also reported that *U. pertusa* grew 16 % faster in the presence of *H. akashiwo* (Cai et al., 2011). The reason for the discrepancy remains unknown.

Due largely to human activities, the atmospheric CO_2 level has reached a value of > 410 ppm, representing a ~48 % increase since the Industrial Revolution. This increase has led to an approximately 30 % increase in ocean acidity and the rate of change is many times faster than anything previously experienced over the last 55 million years, and will accelerate in the coming decades (IPCC, 2013; NOAA, 2019). Ocean acidification can influence both microalgae and macroalgae (Kelly and Hofmann, 2013; Noisette and Hurd, 2018; Hurd et al., 2018). Elevated CO_2 has been shown to enhance the growth of the diatom *S. costatum* in both microcosm (Gao et al., 2012) and mesocosm experiments (Kim et al., 2006). Likewise, elevated CO_2 increased growth of *Ulva* sp. in both laboratory (Gao et al., 2016; Young and Gobler, 2016) and *in situ* (Pajusalu et al., 2013) experiments. Temperature is an essential factor driving the growth of algae and thus the formation of algal blooms (Keesing et al., 2016; Qi et al., 2016). The growth of *S. costatum* has been shown to increase as temperature rises from 20 to 30 °C (Ebrahimi and Salarzadeh, 2016). The growth rate of *Ulva* species also increases with temperature (Mohsen et al., 1973), but higher temperature can also induce more reproduction events, leading to a loss of biomass (Gao et al., 2018a). However, previous studies have focused on monocultures, neglecting the possible interactions between microalgae and macroalgae. To the best of our knowledge, no data regarding how ocean acidification affects the interaction between microalgae and macroalgae under changing temperature regimes have been reported.

In this study, we investigated the physiological properties of a typical red tide alga *S. costatum* (Li et al., 2009) and a green tide alga *U. linza* (Smetacek and Zingone, 2013) that co-occur at low densities in the Yellow Sea but bloom singularly (Tang et al., 2006; Kim et al., 2011; China Marine Disaster Bulletin, 2018), grown in both monoculture and coculture systems at varying CO_2 levels and temperatures, to understand how ocean acidification combined with varying temperature affects the interaction of these two algae and the possible effects on the development of red tides and green tides in the future ocean environment.

2. Material and methods

2.1. Algal collection and experimental design

S. costatum (CCAJ 0101) and *U. linza* (CCAJ 0105) were isolated from the coastal waters (119.3 °E, 34.5 °N) of the Yellow Sea, Jiangsu province of China. A factorial experiment (3 × 2) was conducted to examine the combined effect of ocean acidification and temperature on *S. costatum* and *U. linza* in both monoculture and coculture. Two levels of CO_2 (LC, 400 ppm; HC, 1000 ppm) and three temperatures (12, 18, 24 °C) were set for the experiment. LC and HC represent ambient and future (by the end of this century) CO_2 levels respectively (Gattuso et al., 2015). Three temperatures represent the trend in global warming as well as the seasonal variation in the Yellow Sea (Meehl et al., 2007; Hua et al., 2016; Voosen, 2019). The CO_2 levels were controlled by a CO_2 plant chamber (HP1000G-D, Ruihua Instruments, Wuhan, China). The light was supplied from three sides of the incubators (GXZ-500B, Ningbo, China), with an intensity of 200 μmol photons m^{-2} s^{-1} (L:D = 12:12). *S. costatum* and *U. linza* (about 2 cm in length) were pre-acclimated to the experimental conditions for one week before the experimental culture (Axelsson et al., 1999; Ye and Zhang, 2013).

As for the experimental culture, the initial density for *S. costatum* and *U. linza* was 10,000 cells mL^{-1} and 1 g L^{-1}, respectively, which are values that represent biomass densities during algal blooms. The medium was made of autoclaved natural seawater enriched with f/2 medium to mimic the eutrophic waters for algal blooms and batch culture was conducted with an aeration rate of 300 mL min^{-1} through a 0.22 μm filter (Milipore, America). Cultures were conducted in 1 L balloon flasks containing 900 mL of media in triplicate. Bacteria contamination was minimized by autoclaving media and filtering air. However, the cultures may not be completely axenic as some bacteria may have attached to the surface of *U. linza* and *S. costatum*. The cultures had been terminated when cell numbers of *S. costatum* growing under more than one condition began to decrease and the culture periods lasted 5–7 days for different conditions. Relatively short culture periods may indicate that the coexistence of red tides and green tides cannot last for a long time.

2.2. Seawater carbonate system

The seawater pH was monitored with a pH meter (Eutech Instruments, pH 700, Singapore) and total alkalinity (TA) was determined by acid-base titration (Gao et al., 2018a). The other parameters of the carbonate system were calculated with CO2SYS software based on the known values of TA and pH, using the equilibrium constants of K1 and K2 for carbonic acid dissociation (Roy et al., 1993). The data of carbonate parameters were shown in Table S1.

2.3. Measurement of growth

Cell numbers of *S. costatum* and fresh weight (FW) of *U. linza* at beginning and end of the culture period were measured. Cell numbers were counted by a plankton counter (DSJ-01, Dengxun, Xiamen, China) with microscope (Leica DM500, Germany). Fresh weight was determined by a scale (BS124S, Sartorius, Germany). Daily growth rate (DGR) was calculated using the following formula: $DGR = (W_t/W_0)^{(1/t)} - 1$, where Wt and W_0 are cell density or fresh weight on day T and day 0 respectively.

2.4. Measurement of net photosynthetic oxygen rate and respiration rate

Determination of net photosynthetic oxygen rate (NPR) and dark respiration rate (DRR) was conducted using a Clark-type Oxygen Electrode (Oxygraph +, Hansatech, UK) at the end of the culture period. A cryogenic thermostatic circulator (DHX-2005, China) was used to maintain the temperature. A halogen lamp was used as the light source. The irradiance and temperature conditions were set the same as in the growth incubators. For *S. costatum*, 2 mL of culture medium were added to the chamber and the cell density was about 10^6 cells mL^{-1}. For *U. linza*, approximately 0.005 g (FW) of thalli was transferred to the chamber containing 2 mL culture medium. The samples were placed under the experiment condition for about 1 h to minimize effects of mechanical damage (Gao et al., 2018c). The increase in oxygen content in seawater over a 5 min period was used to estimate NPR, and the

decrease of oxygen content in seawater in darkness within 10 min was defined as DRR. The net photosynthetic rate and dark respiration rate were expressed as pmol O_2 cell^{-1} h^{-1} for *S. costatum* and as μmol O_2 g^{-1} FW h^{-1} for *U. linza*.

2.5. Measurement of photosynthetic pigment

Chl *a* content of samples were measured at the end of the culture period. For *S. costatum*, 25 mL of samples were filtered onto 25 mm GF/F filters (Whatman, UK) and extracted with 8 mL 100 % methanol and stored in darkness for 24 h at 4 °C. The extract was centrifuged (5000 *g* and 4 °C) with a high speed refrigerated centrifuge (Sorvall Biofuge Primo R, Thermo Scientific, US) for 10 min. Chl *a* content was calculated according to the formula of Porra et al. (1989):

$$\text{Chl } a \text{ (g/L)} = 16.29 \times A_{665} - 8.54 \times A_{652},$$

and then converted to pg cell^{-1}.

For *U. linza*, approximately 0.02 g (FW) of thalli were extracted with 8 mL 100 % methanol and stored in darkness for 24 h at 4 °C. The contents of Chl *a* and Chl *b* were calculated according to the formula of Wellburn (1994):

$$\text{Chl } a \text{ (g/L)} = 15.65 \times A_{666} - 7.53 \times A_{653},$$

where A_{666}, A_{665}, A_{653}, and A_{652} are the absorbance wavelength at 666, 665, and 653, and 652 nm, respectively. Values were then converted to mg g^{-1}FW.

2.6. Measurement of nutrients

Nitrate concentration was measured by a rapid spectrophotometric method (Collos et al., 1999; Gao et al., 2018a). Briefly, 2 mL of the culture medium were centrifuged (5000 *g* and 4 °C) with the high speed refrigerated centrifuge for 10 min, and 200 μL of supernatant were measured in a 96-well flat bottom polystyrene microplate with a Multiskan Spectrum (Nultiskan Go, Thermo Scientific, US). Absorbance intensity at 220 nm was used to calculate nitrate concentration by reference to a standard curve.

Phosphate concentration was determined by the phosphomolybdenum blue colorimetry method (Murphy and Riley, 1962; Gao et al., 2018a). Briefly, 5 mL of the culture medium were centrifuged as described above. Afterwards, 1 mL of supernatant was mixed with 5 mL mixed reagent (125 mL of 0.8 M sulphuric acid, 37.5 ml of 0.2 M ammonium molybdate, 75 mL of 0.1 M ascorbic acid solution, and 12.5 mL of 0.004 M potassium antimonyl tartrate solution), reacting at 20 °C for 15 min. Absorbance intensity at 882 nm was determined to calculate the concentration of phosphate by reference to a standard curve.

2.7. Statistical analysis

Data analysis was performed using SPSS v.21 and the data were expressed as means ± standard deviation (SD). The data under every treatment conformed to a normal distribution (Shapiro-Wilk, $P > 0.05$) and the variances could be considered equal (Levene's test, $P > 0.05$). Three-way analysis of variance (ANOVA) was conducted to analyze the effects of temperature, CO_2 and coculture on specific growth rate, net photosynthetic rate, respiration rate, Chl *a* content. Repeated measures ANOVA was used to assess the effects of temperature, CO_2 and coculture on nitrate and phosphate levels in seawater over the culture period. Least significant difference was used for *post hoc* analysis. *P*-values less than 0.05 were considered statistically significant.

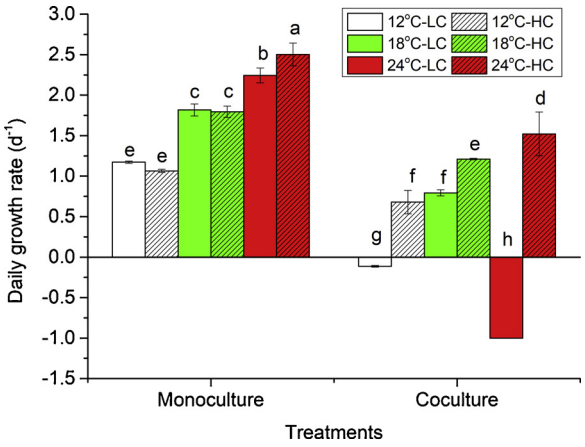

Fig. 1. Daily growth rate of *S. costatum* grown under various CO_2 levels (400 ppm, LC; 1000 ppm, HC) and temperatures. Different letters above the bars represent significant differences among treatments ($P < 0.05$).

3. Results

3.1. Growth under ocean acidification and warming

DGR of *S. costatum* growing alone and with *U. linza* under various CO_2 and temperature conditions were recorded (Fig. 1). CO_2, temperature and *U. linza* had an interactive effect on DGR, any two of them had an interactive and each factor had a significant effect (Table S2). Elevated CO_2 did not affect DGR in monoculture (except for 24 °C) but increased it in coculture. Coculture with *U. linza* significantly reduced DGR of *S. costatum*, particularly for those at LC, leading to negative growth rate at 12 °C and complete death at 24 °C. HC significantly alleviated the inhibitory effect of *U. linza*. Higher temperatures stimulated DGR of *S. costatum* under most conditions and the highest DGR was found at 24 °C and HC in monoculture.

In terms of DGR of *U. linza* (Fig. 2), CO_2 and temperature had an interactive effect on DGR while coculture did not affect it (Table S2). HC increased DGR at 12 °C and 18 °C but decreased it at 24 °C in monoculture. In coculture HC increased DGR at 12 °C, did not affect it 18 °C and decreased it at 24 °C in monoculture. Coculture did not significantly affect DGR except at 18 °C & HC. Compared to 12 °C, higher temperatures increased DGR of *U. linza* at LC but reduced it at HC.

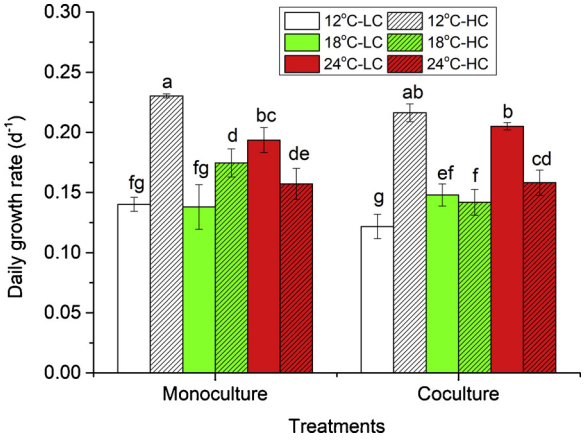

Fig. 2. Daily growth rate of *U. linza* grown under various CO_2 (400 ppm, LC; 1000 ppm, HC) and temperature conditions. Different letters above bars represent significant difference between treatments ($P < 0.05$).

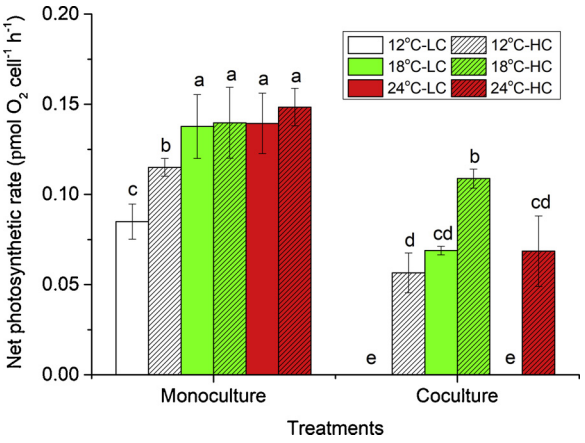

Fig. 3. Net photosynthetic rate of *S. costatum* grown under various CO_2 (400 ppm, LC; 1000 ppm, HC) and temperature conditions. Different letters above bars represent significant difference among treatments ($P < 0.05$).

3.2. Photosynthesis under ocean acidification and warming

The net photosynthetic rates (NPR) of *S. costatum* under various conditions were measured (Fig. 3). Coculture had an interactive effect with CO_2 or temperature, and each factor had a significant effect (Table S3). Elevated CO_2 did not affect NPR in monoculture except for 12 °C but increased it in coculture. Coculture with *U. linza* led to death (24 °C) or nearly death (18 °C) of *S. costatum* at LC and thus the NPR was undetectable. HC significantly alleviated the inhibitory effect of *U. linza* on NPR *in S. costatum*. In monoculture, the higher temperature of 18 °C increased NPR while another 6 °C increase in temperature did not stimulate NPR further; in coculture, highest NPR was found at 18 °C.

As for the NPR of *U. linza* (Fig. 4), CO_2 interacted with temperature or *S. costatum*, and temperature and CO_2 had a significant effect, with the effect of coculture being insignificant (Table S3). HC increased NPR at 18 °C in monoculture, but did not affect it at 18 °C in coculture, 12 or 24 °C. Generally, NPR increased with temperature, with highest value occurring at 24 °C.

3.3. Respiration under ocean acidification and warming

In addition to net photosynthetic rates, dark respiration rates of *S. costatum* (Fig. 5) and *U. linza* (Fig. 6) were also investigated. Three factors interacted with each other on DRR of *S. costatum,* with each having a significant effect (Table S4). In monoculture, higher CO_2 did not affect dark respiration rate; in coculture, higher CO_2 increased DRR at 12 °C and 24 °C but reduced it at 18 °C. Coculture increased DRR at LC & 18 °C and 12 °C & HC. Temperatures did not affect dark respiration rate in monoculture while highest DRR was found at 18 °C for LC and 12 °C for HC in coculture.

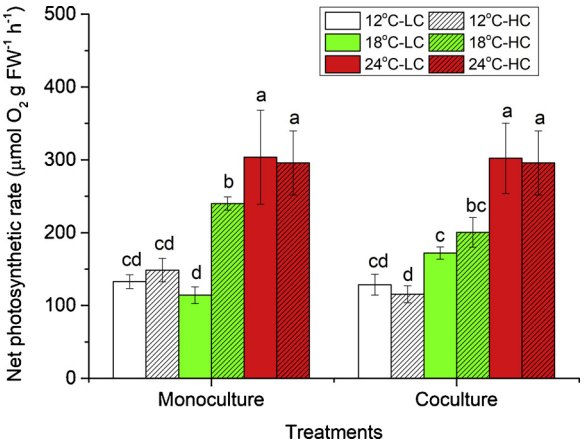

Fig. 4. Net photosynthetic rate of *U. linza* grown under various CO_2 (400 ppm, LC; 1000 ppm, HC) and temperature conditions. Different letters above bars represent significant difference among treatments ($P < 0.05$).

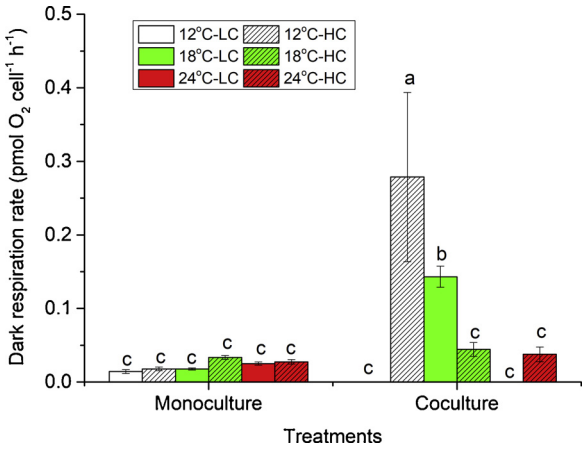

Fig. 5. Dark respiration rate of *S. costatum* grown under various CO_2 (400 ppm, LC; 1000 ppm, HC) and temperature conditions. Different letters above bars represent significant difference among treatments ($P < 0.05$).

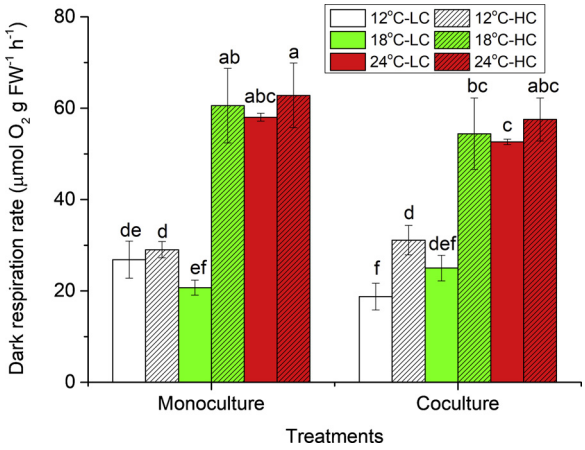

Fig. 6. Dark respiration rate of *U. linza* grown under various CO_2 (400 ppm, LC; 1000 ppm, HC) and temperature conditions. Different letters above bars represent significant difference among treatments ($P < 0.05$).

Dark respiration rates of *S. costatum* in coculture were commonly higher than those in monoculture except for the dead cells. The increased dark respiration rates should be a signal that cells act against the biotic stress from *U. linza*. Unlike those at 12 °C and 24 °C, *S. costatum* at 18 °C in coculture had higher DRR, which also contributed to the higher growth rate. It suggests that the temperature of 18 °C is the optimal for *S. costatum* at LC in coculture after the compromise of itself growth and the inhibitory effect of *U. linza*. That is to say, *S. costatum* had lower a growth rate at 12 °C; although *S. costatum* could have had potentially higher growth rate at 24 °C, it also suffered from more severe inhibition from *U. linza*, leading to the death of cells.

As for *U. linza*, three factors had an interactive effect and CO_2 interacted with temperature on DRR (Table S4). HC did not affect DRR at 24 °C but increased it at 18 °C. At 12 °C, HC did not affect DRR in monoculture but increased it in coculture. Coculture with *S. costatum* did not affect DRR of *U. linza* except for 12 °C & LC. Higher temperatures generally increased DRR, with highest value at 24 °C, which may be related to allelopathic or reproductive compounds. Coculture with *S. costatum* did not increase respiration rate, combined with the results of photosynthesis and growth, indicating that the effect of *S. costatum* on

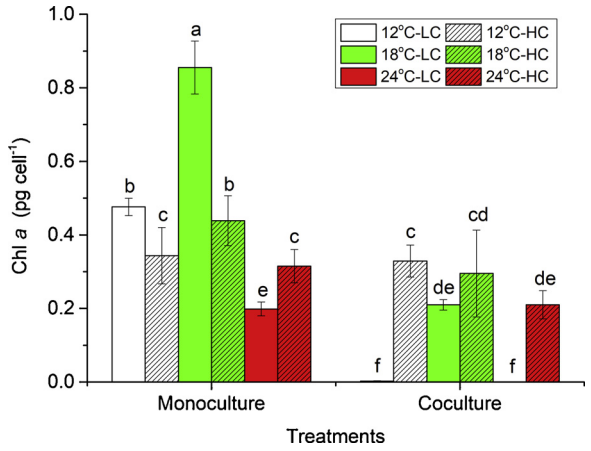

Fig. 7. Content of Chl *a* in *S. costatum* grown under various CO_2 (400 ppm, LC; 1000 ppm, HC) and temperature conditions. Different letters above bars represent significant difference among treatments ($P < 0.05$).

U. linza is negligible.

3.4. Photosynthetic pigments under ocean acidification and warming

The changes of the major photosynthetic pigment, Chl *a*, in *S. costatum* grown under varying temperature and CO_2 conditions were showed in Fig. 7. CO_2, temperature and coculture interacted with each other (Table S5). The cellular content of Chl *a* increased when temperature rose from 12 to 18 °C but decreased when temperature further increased to 24 °C. Higher CO_2 decreased Chl *a* for 12 and 18 °C in monoculture but increased it in coculture. Compared to monoculture, coculture with *U. linza* significantly reduced Chl *a* content except for 12 °C & HC.

The Chl *a* content of *U. linza* was shown in Fig. 8. Temperature and CO_2 had an interactive effect of Chl *a* content in *U. linza* (Table S5). In monoculture, Chl *a* content first increased and then decreased when temperature changes from 12 to 24 °C while Chl *a* content in coculture was not affected by temperature. HC increased Chl *a* content at 24 °C & monoculture but decreased it under the other conditions although the decline was not statistically significant due to multiple comparisons. Coculture with *S. costatum* did not affect Chl *a* except for 24 °C & HC.

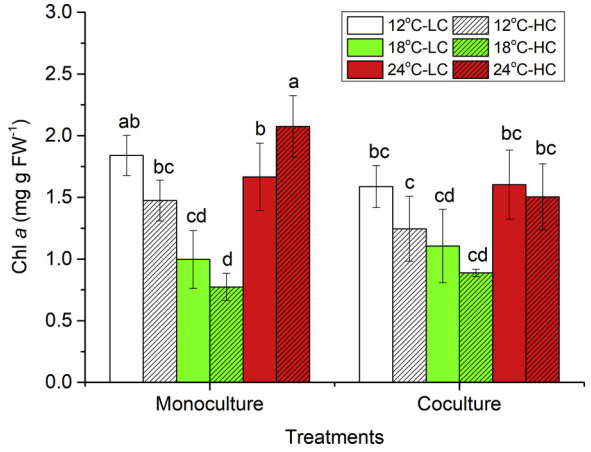

Fig. 8. Content of Chl *a* in *U. linza* grown under various CO_2 (400 ppm, LC; 1000 ppm, HC) and temperature conditions. Different letters above bars represent significant difference among treatments ($P < 0.05$).

4. Discussions

4.1. Effects of ocean acidification and warming on growth

The growth rate of *S. costatum* has been shown to increase with temperatures up to 30 °C (Takabayashi et al., 2006; Kaeriyama et al., 2011; Ebrahimi and Salarzadeh, 2016). The present study also showed a positive effect of temperature (from 12 to 24 °C) on growth of *S. costatum* in monoculture. These findings indicate that ocean warming may stimulate the outbreak of red tides. However, an interesting finding is that coculture with *U. linza* dramatically reduced the growth rate of *S. costatum*, particularly for the highest temperature of 24 °C at which all cells grown at LC began to die on day three. The death could be due to allelopathic effects from *U. linza* since nutrients and dissolved inorganic carbon were not exhausted (Fig. S1 & Table S1). The highest temperature might induce more allelopathic compounds in *U. linza* leading to the strongest inhibitory effect, as found in *Synechococcus* sp. (Śliwińska-Wilczewska et al., 2016). An allelopathic effect on *S. costatum* was also found in other *Ulva* species, such as *U. pertusa* (Ye and Zhang, 2013). Furthermore, the allelopathic effect of *Ulva* species on other bloom-forming microalgae, such as *Heterosigma akashiwo* and *Alexandrium tamarense* (Wang et al., 2007) has been reported. This may explain the fact that green tides can outcompete red tides in some coastal waters in spite of their lower growth rate compared to microalgae. In addition, the shading effect caused by increased biomass of *U. linza* might also contribute to the death of *S. costatum*, and seawater residence time may also affect the competition between these two species (Valiela et al., 1997). Wang et al. (2012) suggested that ammonium toxicity might be another viable reason for the inhibition of *S. costatum* when cultured with effluent from the decomposed *U. prolifera*. In the present study, the initial concentration of ammonium in the media was 2.25 μmol L^{-1} and it would decrease with culture time as nitrate did (Ale et al., 2011). Therefore, ammonium toxicity may not be a possible reason for the inhibition of *S. costatum* in this study. On the other hand, Wang et al. (2012) found that the effluent released by decomposed *U. prolifera* enhanced the growth of *H. akashiwo* and *A. tamarense*. Although decomposition of *Ulva* was not found in the present study, it could occur in the field when green tides decay and thus enhance the growth of some red tide microalgae.

In contrast to the severe inhibitory effect of *U. linza* under LC, the decrease in growth of *S. costatum* was remarkably relieved under HC. *S. costatum* is deemed to have efficient CO_2 concentrating mechanisms (CCMs) while the operation of CCMs is energy-dependent (Raven et al., 2017; Gao et al., 2018b). Elevated CO_2 can down-regulate CCMs and the saved energy could be used by cells to act against the allelopathic inhibition of *U. linza*. Previous studies show that elevated CO_2 alleviated the negative effect of the higher temperature on PSII photoinactivation in the diatoms *Thalassiosira weissflogii* (Gao et al., 2018c) and *Thalassiosira pseudonana* (Yuan et al., 2018), and relieved the toxicity of Cu on growth and photosynthesis in *U. prolifera* (Gao et al., 2017a). Our finding indicates that elevated CO_2 can alleviate the allelopathic inhibition of *Ulva* species on *S. costatum* and reduce the competitive advantage of *Ulva* over microalgae. This is the first report on a positive effect of elevated CO_2 on competition of *S. costatum* with *U. linza*.

Similar to the stimulatory effect on growth of *S. costatum*, higher temperatures also increased growth of *U. linza*. This is consistent with field observation in the Yellow Sea where the sea surface temperature can be 24 °C and the coverage of green tides reaches a peak (Liu et al., 2013). On the other hand, higher temperatures reduced growth of *U. linza* at HC and the optimal temperature is 12 °C for HC. This suggests that elevated CO_2 could reduce the optimal temperature for the growth of *U. linza*. A reason for this is that the combination of higher temperature and elevated CO_2 induced a reproduction event (observed) and thereby reduced vegetative growth. A stimulatory effect of high temperature and CO_2 on reproduction was also found in *U. rigida* (Gao

et al., 2017b, 2018a).

Elevated CO_2 increased growth rate of *U. linza* at 12 °C but did not affect it at 18 °C in coculture and 24 °C. This indicates that the effect of CO_2 on DGR is related to temperature. Under lower temperatures, CCMs run at a lower efficiency due to lower enzyme activity, combined with downregulated CCMs by elevated CO_2, potentially leading to CO_2 limitation for Rubisco (Raven et al., 2011). Therefore, higher CO_2 could stimulate growth of *U. linza* in this study. When temperature rose, elevated CO_2 induced reproduction events and led to the decrease of growth as discussed above. It is worth noting that the response of *Ulva* species to CO_2 and temperature may be species-specific. Different from the present study, previous studies showed that the growth rates of *U. rigida* (Gao et al., 2017b) and *U. lactuca* (Olischläger et al., 2013) were enhanced by elevated CO_2 at 18 °C.

Although coculture significantly reduced growth rate of *S. costatum*, it did not affect growth rate of *U. linza*. From the perspective of ecology strategy, *K*-strategists that are larger in size and have longer life expectancies usually have higher competitive strength compared to *r*-strategists in a stable environment via efficient energy utilization, while *r*-strategists that are generally small and have short life spans typically live in unstable and unpredictable environments via rapid reproduction (Gadgil and Solbrig, 1972; Winkler et al., 2017; Papanikolopoulou et al., 2018). In this study, *U. linza* and *S. costatum* can be seen as *K*-strategists and *r*-strategists respectively (Agrawal, 2011; Papanikolopoulou et al., 2018). *U. linza* could inhibit growth of *S. costatum* via excreting allelopathic compounds under favourable conditions (An et al., 2008) and this may explain why green tides can occur every year in the Yellow Sea and inhibit the outbreak of red tides. On the other hand, *S. costatum* shows competitive advantages when the environments (temperature and CO_2) change.

4.2. Effects of ocean acidification and warming on photosynthesis and pigments

This study indicates that 18–24 °C drops in the optimal temperature range for *S. costatum's* net photosynthetic rate. This finding was consistent with the fact that red tides usually occur in the Yellow Sea from May to September when the surface seawater temperature 18–26 °C (Guo et al., 2015; Park et al., 2015; Hua et al., 2016). Coculture with *U. linza* significantly reduced NPR of *S. costatum*, particularly for those grown at lower CO_2 conditions. Combined with the results of growth, it suggests that the inhibiting effect of *U. linza* on growth of *S. costatum* is related to photosynthesis. Therefore, there is possibility that the allelopathic compounds inhibit growth by hurting photosynthetic apparatus, as found in the case of the macroalga *Gracilaria Tenuistipitata* and the microalga *Prorocentrum micans* (Ye and Zhang, 2013).

Previous studies show that NPR of *Ulva* species commonly increased with temperature (Kim et al., 2011; Zou and Gao, 2014). Our result on *U. linza* confirms this conclusion. However, the increased NPR did not result in an increase in growth of *U. linza* growing at HC as the growth rate of *U. linza* decreased at higher temperatures. We presume the energy generated from increased NPR flow into production of allelopathic or reproductive compounds. Similar to growth, coculture with *S. costatum* did not affect NPR, indicating that *S. costatum* did not pose an effect on photosynthetic apparatus of *U. linza*.

Higher CO_2 usually decreases pigment content of algae which avoid the overexcitation of electron transport under higher CO_2 conditions, which is termed as pigment economy (Gordillo et al., 1998; Gao et al., 2016). This phenomena was also found in *S. costatum* in monoculture (except for 24 °C) but increased it in coculture. On the other hand, elevated CO_2 enhanced Chl *a* content in coculture, which was mainly caused by a dramatic decrease at LC. Chl *a* content of *S. costatum* was reduced to a very low level and even undetectable at LC in coculture. This may be caused by the compounds released by *U. linza* because a previous study has shown that allelopathic compound from *U. pertusa* can harm the oxygen-evolving complex and thus inhibit photosynthesis of *S. costatum* (Ye and Zhang, 2013). Our result suggests that apart from the harm to oxygen-evolving complex, allelopathic compounds from *Ulva* species can inhibit photosynthesis and growth of *S. costatum* via destroying photosynthetic pigment. This conclusion needs confirmation by further studies since allelopathic compounds were not directly measured in the present study.

5. Conclusions

Harmful algal blooms, including red tides and green tides, are on the rise due mainly to increased eutrophication (Bibak and Hosseini, 2013; Smetacek and Zingone, 2013). Meanwhile, continuous CO_2 emission is causing ocean warming and acidification. Previous studies have ignored the interaction of these algal blooms under the context of climate change, although they can occur in the same zones. Our study investigated the combined impacts of ocean acidification and warming on the interaction between red tides and green tides algae for the first time. Higher temperature decreased growth of *U. linza* growing at elevated CO_2 but increased growth of *S. costatum*. Although coculture with *U. linza* significantly reduced growth of *S. costatum* under ambient CO_2 level but elevated CO_2 dramatically alleviate the inhibitory effect of *U. linza*. *Ulva*-dominated green tides occur annually in the Yellow Sea and hamper the outbreak of red tides. These findings indicate that *S. costatum* may have an enhanced advantage over *U. linza* in future warmer and CO_2-enriched oceans, thus altering the current balance between red tides and green tides.'

Declaration of Competing Interest

The authors declare that they have no known competing financial interests or personal relationships that could have appeared to influence the work reported in this paper.

Acknowledgement

This study was supported by the National Key Research and Development Program of China (2018YFD0900703), the Lianyungang Innovative and Entrepreneurial Doctor Program (201702), the Six Talents Peaks in Jiangsu Province (JY- 086) and Priority Academic Program Development of Jiangsu Higher Education Institutions. [CG]

Appendix A. Supplementary data

Supplementary material related to this article can be found, in the online version, at doi:https://doi.org/10.1016/j.hal.2019.101698.

References

Accoroni, S., Percopo, I., Cerino, F., Romagnoli, T., Pichierri, S., Perrone, C., Totti, C., 2015. Allelopathic interactions between the HAB dinoflagellate *Ostreopsis cf. ovata* and macroalgae. Harmful Algae 49 (14), 147–155.

Agrawal, A.A., 2011. Current trends in the evolutionary ecology of plant defence. Funct. Ecol. 25 (2), 420–432.

Ale, M.T., Mikkelsen, J.D., Meyer, A.S., 2011. Differential growth response of *Ulva lactuca* to ammonium and nitrate assimilation. J. Appl. Phycol. 23 (3), 345–351.

An, Z., Wang, Z.Y., Li, F.M., Tian, Z.J., Hu, H.Y., 2008. Allelopathic inhibition on red tide microalgae *Skeletonema costatum* by five macroalgal extracts. Front. Environ. Sci. Eng. China 2 (3), 297–305.

Anderson, D.M., 2009. Approaches to monitoring, control and management of harmful algal blooms (HABs). Ocean Coast. Manag. 52, 342–347.

Axelsson, L., Larsson, C., Ryberg, H., 1999. Affinity, capacity and oxygen sensitivity of two different mechanisms for bicarbonate utilization in *Ulva lactuca* L. (Chlorophyta). Plant Cell Environ. 22 (8), 969–978.

Besterman, A.F., Pace, M.L., 2018. Do Macroalgal mats impact microphytobenthos on mudflats? Evidence from a meta-analysis, comparative survey, and large-scale manipulation. Estuar. Coast. 41 (8), 2304–2316.

Bibak, M., Hosseini, S.A., 2013. Review ways to control harmful algal bloom (HAB). World J. Fish Mar. Sci. 5 (1), 42–44.

Bourne, Y., Radić, Z., Aráoz, R., Talley, T.T., Benoit, E., Servent, D., Taylor, P., Molgó, J., Marchot, P., 2010. Structural determinants in phycotoxins and AChBP conferring high affinity binding and nicotinic AChR antagonism. Proc. Natl. Acad. Sci. U. S. A.

107 (13), 6076–6081.
China Marine Disaster Bulletin, 2018. Division of Marine Early Warning and Monitoring. Ministry of Natural Resources of the People's Republic of China.
Cai, H.J., Li, B., Liu, C.F., 2011. The Interaction between *Ulva pertusa* (Chlorophyta) and *Heterosigma akashiwo* (Xanthophyta) and its responses to UV-B radiation. 2011. Internat. Symp.Water Resource Environment. Prot. 4, 2575–2578.
Collos, Y., Mornet, F., Sciandra, A., Waser, N., Laeson, A., Harrison, P.J., 1999. An optical method for the rapid measurement of micromolar concentrations of nitrate in marine phytoplankton cultures. J. Plant Physiol. 11 (2), 179–184.
Ebrahimi, E., Salarzadeh, A., 2016. The effect of temperature and salinity on the growth of *Skeletonema costatum* and *Chlorella capsulata* in vitro. Internat. J. Life Sci. 10 (1), 40–44.
Fletcher, R.L., 1996. The occurrence of "green tides"-a review. In: Schramm, W., Nienhuis, P.H. (Eds.), Marine Benthic Vegetation. Springer, Berlin, pp. 7–43.
Fong, P., Donohoe, R.M., Zedler, J.B., 1993. Competition with macroalgae and benthic cyanobacterial mats limits phytoplankton abundance in experimental microcosms. Mar. Ecol. Prog. Ser. 100, 97–102.
Gadgil, M., Solbrig, O.T., 1972. The concept of R-and K-selection: evidence from wild flowers and some theoretical considerations. Am. Nat. 106 (947), 14–31.
Gao, G., Liu, Y.M., Li, X.S., Feng, Z.H., Xu, J.T., 2016. An ocean acidification acclimatised green tide alga is robust to changes of seawater carbon chemistry but vulnerable to light stress. PLoS One 11 (12), e0169040.
Gao, G., Clare, A.S., Rose, C., Caldwell, G.S., 2017b. Eutrophication and warming-driven green tides (*Ulva rigida*) are predicted to increase under future climate change scenarios. Mar. Pollut. Bull. 114 (1), 439–447.
Gao, G., Clare, A.S., Rose, C., Caldwell, G.S., 2018a. *Ulva rigida* in the future ocean: potential for carbon capture, bioremediation and biomethane production. Gcb Bioenergy 10 (1), 39–51.
Gao, G., Liu, Y.M., Li, X.S., Feng, Z.H., Feng, Z.H., Xu, Z.G., Wu, H.L., Xu, J.T., 2017a. Expected CO_2-induced ocean acidification modulates copper toxicity in the green tide alga *Ulva prolifera*. Environ. Exp. Bot. 135 (10), 63–72.
Gao, G., Shi, Q., Xu, Z.G., Xu, J.T., Campbell, D.A., Wu, H.Y., 2018c. Global warming interacts with ocean acidification to alter PSII function and protection in the diatom Thalassiosira weissflogii. Environ. Exp. Bot. 147, 95–103.
Gao, G., Xia, J.R., Yu, J.T., Fan, J.L., Zeng, X.P., 2018b. Regulation of inorganic carbon acquisition in a red tide alga (*Skeletonema costatum*): the importance of phosphorus availability. Biogeosciences 15 (16), 4871–4882.
Gao, K.S., Xu, J.T., Gao, G., Li, Y.H., Hutchins, D.A., Huang, B.Q., Wang, L., Zheng, Y., Jin, P., Cai, X.N., Häder, D.P., Wei, L., Xu, K., Liu, N.N., Riebesell, U., 2012. Rising CO_2 and increased light exposure synergistically reduce marine primary productivity. Nat. Clim. Change 2 (7), 519–523.
Gattuso, J.P., Magnan, A., Billé, R., Cheung, W.W., Howes, E.L., Joos, F., Allemand, D., Bopp, L., Cooley, S.R., Eakin, C.M., Hoegh-Guldberg, O., 2015. Contrasting futures for ocean and society from different anthropogenic CO_2 emissions scenarios. Science 349 (6243) aac4722.
Gordillo, F.J., Jiménez, C., Figueroa, F.L., Niell, F.X., 1998. Effects of increased atmospheric CO_2 and N supply on photosynthesis, growth and cell composition of the cyanobacterium *Spirulina platensis* (*Arthrospira*). J. Appl. Phycol. 10 (5), 461–469.
Guo, H., Ding, D.W., Lin, F.A., Guan, C.J., 2015. Characteristics and patterns of red tide in China coastal waters during the last 20a. Adv. Mar. Sci. 33 (4), 547–558.
Hua, C.J., Wu, Y., Zhang, H., Cui, X.S., Yang, S.L., 2016. Analysis on the seasonal variability of sea surface temperature in the east the yellow sea in 2014. Fish. Inform. Strateg. 31, 193–205.
Hurd, C.L., Lenton, A., Bronte, T., Philip, W.B., 2018. Current understanding and challenges for oceans in a higher-CO_2 world. Nat. Clim. Change 8, 686–694.
IPCC, et al., 2013. Climate change 2013: the physical science basis. In: Stocker, T.F., Qin, D.H., Plattner, G.K. (Eds.), Working Group I Contribution to the Fifth Assessment Report of the Intergovernmental Panel on Climate Change. Cambridge University Press, New York, pp. 6–10.
Kaeriyama, H., Katsuki, E., Otsubo, M., Yamada, M., Ichimi, K., Tada, K., Harrison, P.J., 2011. Effects of temperature and irradiance on growth of strains belonging to seven *Skeletonema* species isolated from Dokai Bay, Southern Japan. Eur. J. Phycol. 46 (2), 113–124.
Kelly, M.W., Hofmann, G.E., 2013. Adaptation and the physiology of ocean acidification. Funct. Ecol. 27 (4), 980–990.
Kirkpatrick, B., Fleming, L.E., Squicciarini, D., Backer, L.C., Clark, R., Abraham, W., Benson, J., Cheng, Y.S., Johnson, D., Pierce, R., 2004. Literature review of Florida red tide: implications for human health effects. Harmful Algae 3, 99–115.
Keesing, J.K., Liu, D.Y., Shi, Y.J., Wang, Y.J., 2016. Abiotic factors influencing biomass accumulation of green tide causing *Ulva* spp. on *Pyropia*culture rafts in the Yellow Sea, China. Mar. Pollut. Bull. 105 (1), 88–97.
Kim, J.H., Kang, E.J., Park, M.G., Lee, B.G., Kim, K.Y., 2011. Effects of temperature and irradiance on photosynthesis and growth of a green-tide-forming species (*Ulva linza*) in the Yellow Sea. J. Appl. Phycol. 23 (3), 421–432.
Kim, J.M., Lee, K., Shin, K., Kang, J.H., Lee, H.W., Kim, M., Jang, P.G., Jang, M.C., 2006. The effect of seawater CO_2 concentration on growth of a natural phytoplankton assemblage in a controlled mesocosm experiment. Limnol. Oceanogr. 51 (4), 1629–1636.
Li, C.Q., Zhu, B.B., Chen, H., Liu, Z.X., Cui, B.M., Wu, J.R., Li, B., Yu, H.C., Peng, M., 2009. The relationship between the *Skeletonema costatum* red tide and environmental factors in Hongsha Bay of Sanya, South China Sea. J. Coastal. Res. 25 (3), 651–658.
Liu, D.Y., Keesing, J.K., He, P.M., Wang, Z.L., Shi, Y.J., Wang, Y.Y., 2013. The world's largest macroalgal bloom in the Yellow Sea, China: formation and implications. Estuar. Coast. Shelf Sci. 129 (2), 2–10.
Meehl, G., Stocker, T., Collins, W., et al., 2007. Climate Change 2007: the Physical Science Basis: Contribution of Working Group I to the Fourth Assessment Report of the Intergovernmental Panel on Climate Change. Cambridge University Press, U.K, pp. 747–846.
Mohsen, A.F., Nasr, A.H., Metwalli, A.M., 1973. Effect of temperature variations on growth, reproduction, amino acid synthesis, fat and sugar content in *Ulva fasciata* delile plants. Hydrobiologia 42 (4), 451–460.
Morabito, S., Silvestro, S., Faggio, C., 2018. How the marine biotoxins affect human health. Nat. Prod. Res. 32 (6), 621–631.
Murphy, J., Riley, J.P., 1962. A modified single solution method for the determination of phosphate in natural waters. Anal. Chim. Acta 27 (6), 31–36.
Nan, C.R., Zhang, H.Z., Zhao, G.Q., 2004. Allelopathic interactions between the macroalga *Ulva pertusa* and eight microalgal species. J. Sea Res. 52 (4), 259–268.
National Oceanic and Atmospheric Administration Website, https://www.co2.earth, USA.
Noisette, F., Hurd, C., 2018. Abiotic and biotic interactions in the diffusive boundary layer of kelp blades create a potential refuge from ocean acidification. Funct. Ecol. 32 (5), 1329–1342.
Olischläger, M., Bartsch, I., Gutow, L., Wiencke, C., 2013. Effects of ocean acidification on growth and physiology of *Ulva lactuca* (Chlorophyta) in a rockpool-scenario. Phycol. Res. 61, 180–190.
Pajusalu, L., Martin, G., Põllumäe, A., Paalme, T., 2013. Results of laboratory and field experiments of the direct effect of increasing CO_2 on net primary production of macroalgal species in brackish-water ecosystems. Proc. Estonian Acad. Sci. Biol. Ecol. 62 (2), 148–154.
Papanikolopoulou, L.A., Smeti, E., Roelke, D.L., Dimitrakopoulos, P.G., Kokkoris, G.D., Danielidis, D.B., Spatharis, S., 2018. Interplay between r-and k-strategists leads to phytoplankton underyielding under pulsed resource supply. Oecologia 186 (3), 755–764.
Park, K.A., Lee, E.Y., Chang, E., Hong, S., 2015. Spatial and temporal variability of sea surface temperature and warming trends in the Yellow Sea. J. Mar. Syst. 143 (3), 24–38.
Porra, R.J., Thompson, W.A., Kriedemann, P.E., 1989. Determination of accurate extinction coefficients and simultaneous equations for assaying chlorophylls *a* and *b* extracted with four different solvents: verification of the concentration of chlorophyll standards by atomic absorption spectroscopy. Biochim. Biophys. Acta 975 (3), 384–394.
Qi, L., Hu, C., Xing, Q., Shang, S., 2016. Long-term trend of *Ulva prolifera* blooms in the Western Yellow Sea. Harmful Algae 58, 35–44.
Raven, J.A., Beardall, J., Sánchez-Baracaldo, P., 2017. The possible evolution and future of CO_2-concentrating mechanisms. J. Exp. Bot. 68 (14), 3701–3716.
Raven, J.A., Giordano, M., Beardall, J., Maberly, S.C., 2011. Algal and aquatic plant carbon concentrating mechanisms in relation to environmental change. Photosynth. Res. 109 (1–3), 281–296.
Roy, R.N., Roy, L.N., Vogel, K.M., Porter- Moore, C., Pearson, T., Good, C.E., Millero, F.J., Campbell, D.M., 1993. The dissociation constants of carbonic acid in seawater at salinities 5 to 45 and temperatures 0 to 45°C. Mar. Chem. 44 (2–4), 249–267.
Shumway, S.E., Allen, S.M., Boersma, P.D., 2003. Marine birds and harmful algal blooms: sporadic victims or under-reported events? Harmful Algae 2 (1), 1–17.
Smetacek, V., Zingone, A., 2013. Green and golden seaweed tides on the rise. Nature 504 (7478), 84–88.
Smith, D.W., Horne, A.J., 1988. Experimental measurement of resource competition between planktonic microalgae and macroalgae (seaweeds) in mesocosms simulating the San Francisco Bay-Estuary, California. Hydrobiologia 159 (3), 259–268.
Śliwińska-Wilczewska, S., Pniewski, F., Latała, A., 2016. Allelopathic activity of the picocyanobacterium *Synechococcus* sp. Under varied light, temperature, and salinity conditions. Int. Rev. Hydrobiol. 101 (1–2), 69–77.
Tang, D., Di, B., Wei, G., Ni, I.H., Wang, S., 2006. Spatial, seasonal and species variations of harmful algal blooms in the South Yellow Sea and East China Sea. Hydrobiologia 568 (1), 245–253.
Turner, J.T., Tester, P.A., Hansen, P.J., 1998. Interactions between toxic marine phytoplankton and metazoan and protistan grazers. In: Anderson, D.M., Cembella, A.D., Hallegraeff, G.M. (Eds.), Physiological Ecology of Harmful Algal Blooms. NATO ASI Series 41. Springer, Berlin Heidelberg New York, pp. 453–474.
Takabayashi, M., Lew, K., Johnson, A., Marchi, A.L., Dugdale, R., Wilkerson, F.P., 2006. The effect of nutrient availability and temperature on chain length of the diatom, *Skeletonema costatum*. J. Plankton Res. 28 (9), 831–840.
Voosen, P., 2019. New climate models forecast a warming surge. Science 364, 222–223.
Wang, C., Yu, R.C., Zhou, M.J., 2012. Effects of the decomposing green macroalga *Ulva* (*Enteromorpha*) *prolifera* on the growth of four red-tide species. Harmful Algae 16, 12–19.
Wang, R.J., Hui, X., Zhang, P.Y., Liang, Q., Cai, H.J., Tang, X.X., 2007. Allelopathic effects of *Ulva pertusa*, *Corallina pilulifera* and *Sargassum thunbergii* on the growth of the dinoflagellates *Heterosigma akashiwo* and *Alexandrium tamarense*. J. Appl. Phycol. 19 (2), 109–121.
Wellburn, A.R., 1994. The spectral determination of chlorophylls *a* and *b*, as well as total carotenoids, using various solvents with spectrophotometers of different resolution. J. Plant Physiol. 144 (3), 307–313.
Winkler, M.K., Boets, P., Hahne, B., Goethals, P., Volcke, E.I., 2017. Effect of the dilution rate on microbial competition: r-strategist can win over K-strategist at low substrate concentration. PLoS One 12 (3), e0172785.
Xia, B., Ma, S., Cui, Y., Chen, B., Chen, J., Song, Y., Mao, Y., 2009. Distribution of temperature, salinity, dissolved oxygen, nutrients and their relationships with green tide in *Enteromorpha prolifera* outbreak area of the Yellow Sea. Progr. Fish. Sci. 30, 94–101.
Ye, C.P., Zhang, M.C., 2013. Allelopathic inhibitory effects of the dried macroalga *Ulva pertusa* on the photosynthetic activities of red tide-causing microalga *Skeletonema costatum*. Adv. Mater. Res. 726, 29–34.
Ye, N.H., Zhang, X.W., Mao, Y.Z., Liang, C.W., Xu, D., Zou, J., Zhuang, Z.M., Wang, Q.Y.,

2011. 'Green tides' are overwhelming the coastline of our blue planet: taking the world's largest example. Ecol. Res. 26, 477–485.
Young, C.S., Gobler, C.J., 2016. Ocean acidification accelerates the growth of two bloom-forming macroalgae. PLoS One 11 (5), e0155152.
Yuan, W.B., Gao, G., Shi, Q., Xu, Z.G., Wu, H.Y., 2018. Combined effects of ocean acidification and warming on physiological response of the diatom *Thalassiosira pseudonana* to light challenges. Mar. Environ. Res. 135 (8), 63–69.
Zhang, Y., et al., 2019. *Ulva prolifera* green tide outbreaks and their environmental impact in the Yellow Sea, China. Sci. Rev. 6 (4), 825–838.
Zou, D.H., Gao, K.S., 2014. The photosynthetic and respiratory responses to temperature and nitrogen supply in the marine green macroalga *Ulva conglobata* (Chlorophyta). Phycologia 53 (1), 86–94.